THE JOURNAL OF PHYSICAL CHEMISTRY Letters

Letter

pubs.acs.org/JPCL

Nanodroplet Transport on Vibrated Nanotubes

John T. Russell,[†] Boyang Wang,[†] and Petr Král*[,†,‡]

[†]Department of Chemistry, University of Illinois at Chicago, Chicago, Illinois 60607, United States

[‡]Department of Physics, University of Illinois at Chicago, Chicago, Illinois 60607, United States

Web-Enhanced Feature

ABSTRACT: We show by molecular dynamics simulations that water nanodroplets can be transported along and around the surfaces of vibrated carbon nanotubes. In our simulations, a nanodroplet with a diameter of ∼4 nm is adsorbed on a (10,0) single-wall carbon nanotube, which is vibrated at one end with a frequency of 208 GHz and an amplitude of 1.2 nm. The generated linearly polarized transverse acoustic waves pass linear momentum to the nanodroplet, which becomes transported along the nanotube with a velocity of ∼30 nm/ns. When circularly polarized waves are passed along the nanotubes, the nanodroplets rotate around them and eventually become ejected from their surfaces when their angular velocity is ∼50 rad/ns.

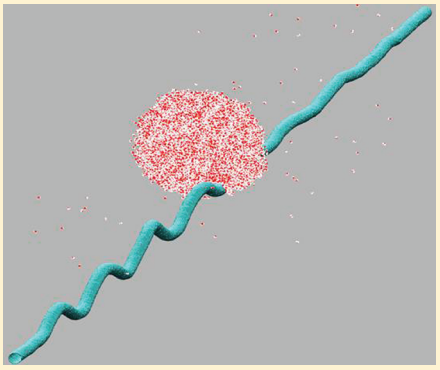

SECTION: Dynamics, Clusters, Excited States

Carbon nanotubes[1] (CNTs) can serve as nanoscale railroads for transport of materials, due to their linear structure, mechanical strength, slippery surfaces, and chemical stability.[2] For example, electric currents passing through CNTs can drag atoms/molecules intercalated/adsorbed on CNTs.[3−5] Polar molecules and ions adsorbed on CNT surfaces can also be dragged by ionic solutions passing through the tubes.[6−8] Recently, nanoparticles[9,10] and nanodroplets[11,12] have been dragged along CNTs by hot phonons in thermal gradients. Analogously, breathing[13] and torsional[14] coherent phonons can pump fluids inside CNTs.

Materials adsorbed on macroscopic solid-state surfaces can be transported by surface acoustic waves (SAWs).[15] This method has many practical applications, such as conveyor belt technologies,[16] ultrasonic levitation of fragile materials,[17] slipping of materials on tilted surfaces,[18,19] threading of cables inside tubes,[20] and droplet delivery in microfluidics.[21−25]

In this work, we examine the possibility of using SAW at the nanoscale. We use classical molecular dynamics (MD) simulations to model transport (drag) of water nanodroplets on the surface of CNTs by coherent acoustic waves. Such coherent vibrations might be generated by piezo-electric generators.[26,27] Analogous to coherent control of molecules by light,[28] specialized pulses of coherent phonons might also be used in precise manipulation of materials.

Model System. Our model systems are formed by nanodroplets consisting of a number, N_w, of water molecules adsorbed at T = 300 K on the (10,0) CNT, and transported along/around its surface by coupling to coherent transversal acoustic (TA) phonon waves, as shown in Figure 1. We simulate the systems with classical MD simulations, using NAMD,[29] with the CHARMM27 force field[30] with the TIP3P model for water molecules in the nanodroplet, and VMD[31] for visualization and analysis. The nanodroplets couple to the CNT by van der Waals (vdW) forces, described in CHARMM with the Lennard-Jones potential energy[32]

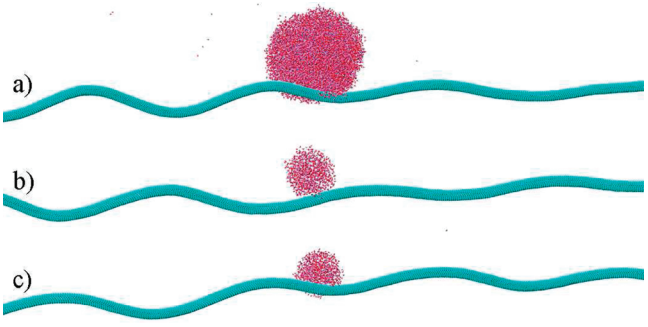

Figure 1. Nanodroplets of (a) N_w = 10 000 and (b) N_w = 1000 waters adsorbed on the (10,0) CNT and transported along its surface by the linearly polarized TA vibrational wave with an amplitude of A = 1.2 (T = 300 K). (c) A nanodroplet of N_w = 1000 adsorbed on the same CNT rotated (and translated) around its surface by a circularly polarized vibrational wave of A = 0.75 nm (see Movies 1 and 2).

$$V_{LJ}(r_{ij}) = \varepsilon_{ij}\left[\left(\frac{R_{\min,ij}}{r_{ij}}\right)^{12} - 2\left(\frac{R_{\min,ij}}{r_{ij}}\right)^{6}\right] \quad (1)$$

Received: December 7, 2011
Accepted: January 10, 2012
Published: January 10, 2012

Here, $\varepsilon_{ij} = (\varepsilon_i\varepsilon_j)^{1/2}$ is the depth of the potential well, $R_{\min,ij} = 1/2\,(R_{\min,i} + R_{\min,j})$ is the equilibrium vdW distance, and r_{ij} is the distance between a CNT atom and a water atom.

The edge atoms at one of the ends of the 450 nm long CNT are fixed. At this end the tube is also oscillated. To prevent the CNT translation, four dummy atoms are placed in its interior at both ends. Otherwise, the tube is left free. A small Langevin damping[33] of 0.01 ps^{-1} is applied to the system to continuously thermalize it, while minimizing the unphysical loss of momenta;[6] the time step is 2 fs. At the two CNT ends, two regions with high damping of 10 ps^{-1} are established to absorb the vibrational waves. One region (35 nm long) is close to the generation point, and the other (180 nm long) is at the other CNT end. We model the systems in a NVT ensemble (periodic cell of 15 × 15 × 470 nm^3).

Nanodroplet Transport by Linearly Polarized Waves. The vibrational waves are generated at one CNT end by applying a periodic force (orthogonal to its axis), $F = F_0 \sin(\omega t)$, on the carbon atoms separated 43−48 nm from the CNT end. This generates a linearly polarized TA vibration wave, $A_y(t) = A \sin(\omega t)$, where $\omega \approx 208$ GHz, $k = 2\pi/\lambda \approx 0.157$ nm^{-1}, and $A \approx 0.3$−2.1 nm for $F_0 = 0.6948$−5.558 pN/atom. The TA waves propagate along the nanotube with a velocity of $v_{vib} = \omega/k \approx 1{,}324$ nm/ns, scatter with the nanodroplet, and become absorbed at the tube ends. In our simulations, we let the wave pass around the droplet for a while and then evaluate its average steady-state translational, v, and angular, ω_d, velocities.

In Figure 2, we show the (linear) velocities of nanodroplets with N_w = 1000 and 10 000 water molecules as a function of the vibrational amplitude, A. The data are obtained by averaging the droplet motion over trajectories of the length of $t \approx 7.2$ ns. We can see that the 10-times smaller droplet moves about 15-times faster for the same driving conditions. At small amplitudes ($A < 1.2$ nm) the velocities roughly depend quadratically on the driving amplitude. At larger amplitudes ($A > 1.2$ nm) they gain a linear dependence.

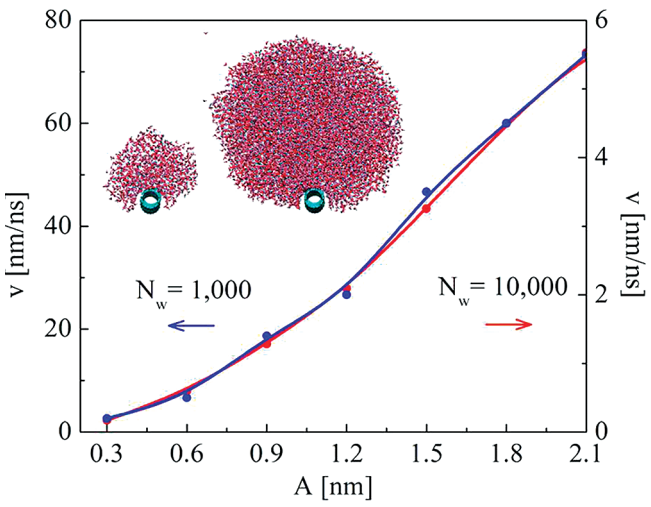

Figure 2. The velocity of nanodroplets with N_w = 1000 and 10 000 waters shown as a function of the amplitude, A, of the linearly polarized wave with the frequency of ω = 208 GHz. (Inset) The adsorbed nanodroplets viewed in the CNT axis.

The nanodroplet is transported by absorbing a momentum from the vibrational wave. Its steady-state motion is stabilized by frictional dissipation of the gained momentum with the nanotube, which carries it away through the highly damped and fixed atoms. In the first approximation, the droplet motion might be described by the Boltzmann equation. In the steady state, obtained when a wave of a constant amplitude is passed through the CNT, the momentum of the droplet averaged over a short time (50 ps) is constant. Then, the constant driving force acting on the droplet, $\dot{P}_{drive}$, is equal the friction force, $\dot{P}_{friction}$, between the droplet and the CNT[32] (linear motion, vectors omitted):

$$\dot{P}_{drive} = \int pF(r)\frac{\partial f}{\partial p}\,dr\,dp = \int p\left(\frac{\partial f}{\partial t}\right)_{coll} dr\,dp = \dot{P}_{friction} \quad (2)$$

Here, $f(r,p)$ is the position and momentum distribution function of the waters in the nanodroplet (normalized to N_w), and $F(r)$ is the force acting on each of the waters at r. The collision term $(\partial f/\partial t)_{coll}$ describes scattering of waters with each other and the CNT, where the last option causes the droplet to relax its momentum.[34] In the approximation of the momentum relaxation time,[35] τ_p, the damping term can be described as

$$\int p\left(\frac{\partial f}{\partial t}\right)_{coll} dr\,dp = \int p\frac{f - f_0}{\tau_p}\,dr\,dp \approx \frac{P_{droplet}}{\tau_p} \quad (3)$$

where $P_{droplet}$ is the steady-state average momentum of the nanodroplet.[6,7]

As the acoustic wave propagates along the CNT, it carries the momentum density,[36]

$$g(t, x) = \mu\omega kA^2[1 + \cos(2kx - 2\omega t)] \quad (4)$$

where μ is the CNT mass per unit length and the other symbols are the same as before. Assuming, for simplicity, that the momentum density of the wave is fully passed to the droplet (only approximately true, as seen in Figure 1), we obtain

$$\dot{P}_{drive} = \frac{1}{2}\mu\omega^2A^2 = \frac{P_{droplet}}{\tau_p} \quad (5)$$

Equation 5 shows that the droplet velocity scales as

$$v_t = \frac{P_{droplet}}{m} \approx \frac{A^2\tau_p}{m} \quad (6)$$

Moreover, the momentum relaxation time, $\tau_p \approx S^{-1}$, can be assumed to scale inversely with the contact area, S, between the droplet and the CNT, due to friction. The 15 times larger velocity of the 10 times smaller droplet with a smaller contact area matches our expectations from eq 6. The quadratic dependence of the droplet velocities on the driving amplitude, A, shown in Figure 2, also roughly agrees with eq 6.

Nanodroplet Transport by Circularly Polarized Waves. Next, we simulate transport of nanodroplets with N_w = 1000 and 2000 waters, adsorbed on the (10,0) CNT, by circularly polarized TA waves. Application of the force of $\mathbf{F}(t) = (F_x,F_y) = F_0(\sin(\omega t), \cos(\omega t))$, $F_0 = 0.4864 - 2.084$ pn/atom, on the same C atoms as before generates a circularly polarized wave, $\mathbf{A}(t) = (A_x,A_y) = A(\sin(\omega t), \cos(\omega t))$, where $A \approx 0.21 - 0.75$ nm, $\omega \approx 208$ GHz, and $k \approx 0.157$ nm^{-1}. The circularly polarized TA waves carry both linear and angular momenta and pass them to the nanodroplets, which are transported along the CNT and rotated around it.

In Figure 3, we plot the translational, v, and the angular, ω_d, velocities of the nanodroplets as a function of the wave amplitude, A. For N_w = 1000, ω_d rapidly grows with A until

dx.doi.org/10.1021/jz201614m | J. Phys. Chem. Lett. 2012, 3, 353−357

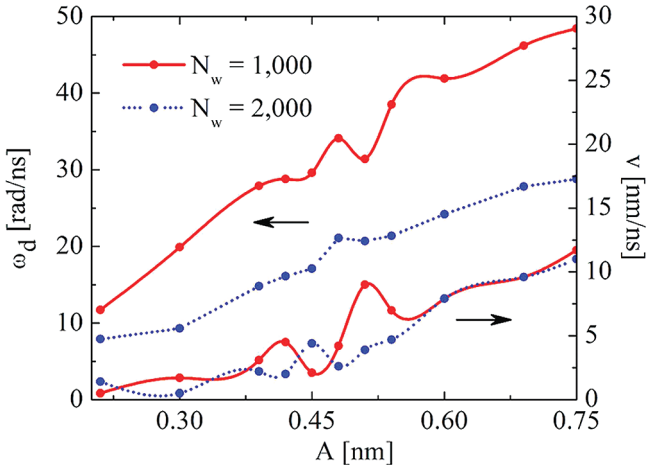

Figure 3. The average translational v and angular ω_d velocities of water nanodroplets with N_w = 1000 and 2000 as a function of the wave amplitude, A, when driven by circularly polarized waves.

$\omega_{d,max} \approx$ 50.5 rad/ns, where the droplet is ejected from the CNT surface, due to large centrifugal forces. The larger droplet rotates with ∼30−40% smaller angular velocity, in analogy to the situation in a linear transport. At A = 0.4−0.6 nm, both the linear and angular velocities show certain resonant features for both droplets. At these amplitudes of the circular waves, the coupling to the droplets can be dramatically altered, since the wave amplitudes are similar to the droplet sizes. Interestingly, the translational velocities, v, are very similar for both droplets. This might be due to better transfer of linear momentum to the larger droplet from circularly polarized waves.

We can perform similar analysis of the angular momentum passage from the circular wave to the droplet and back to the CNT, like we did for the linear momentum in eqs 2−6. In a steady state, obtained when a circularly polarized wave of a constant amplitude is passed through the CNT, the average angular momentum of the droplet around the (equilibrium position of) CNT axis is constant. The driving momentum of force, $\dot{L}_{drive}$, acting on the droplet is equal to its friction counterpart, $\dot{L}_{friction}$, acting between the droplet and the CNT.[37] Assuming that the whole angular momentum density of the wave is passed to the droplet and using the approximation of the angular momentum relaxation time, we find

$$\dot{L}_{drive} = f(\mu, \omega, A) = \frac{L_{droplet}}{\tau_L} = \frac{I\omega_d}{\tau_L} = C \qquad (7)$$

where $f(\mu,\omega,A)$ is the angular momentum density (size) of the circularly polarized wave, I is the droplet moment of inertia with respect to the (equilibrium) CNT axis, and τ_L is the angular momentum relaxation time. In the steady state, the average rates of driving and damping are constant, as shown by C. The moment of inertia is $I = \sum_{i=1}^{n} m_w r_i^2 \propto N_w$, where m_w is the mass of a water molecule, and r_i is the distance of each water molecule from the (equilibrium) CNT axis. Using this I in eq 7, we find that $w_d \propto N_w^{-1}$, in rough agreement with Figure 3.

We can also describe the droplet ejection. The angular motion of the droplet around the (equilibrium) CNT axis generates a radial centrifugal force, $F_c = m\omega_d^2/h$, where m is the droplet mass and h is its distance from the (equilibrium) CNT axis. When the centrifugal force exceeds the vdW force that binds the droplet to the CNT, the droplet is ejected.[38] This happens for the centrifugal force of F_c = 150.2 pN, obtained for A = 0.9 nm, ω_d = 50.5 rad/ns, and h = 19.7 Å. We can roughly estimate the vdW binding forces for a relaxed water droplet coupled to a frozen CNT by applying a fictitious force on the droplet in the direction orthogonal to the CNT axis. This gives a force of $F_{vdW} \approx$ 229 pN. In the presence of droplet rotation around the CNT, the vdW forces should be smaller, since the droplet has a smaller contact with the CNT, i.e., $F_c \approx F_{vdW}$.

In order to better understand the droplet−CNT dynamics, we present in Figure 4 the time-dependent motion of the

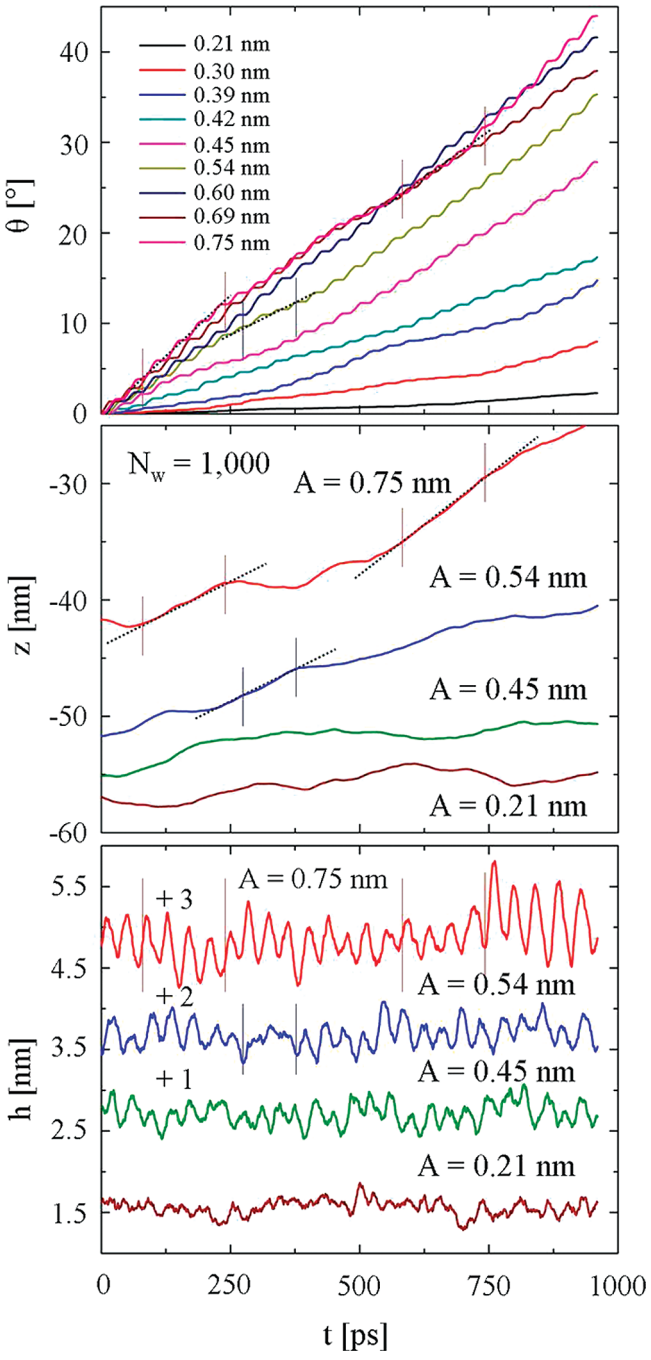

Figure 4. Time-dependent angle of rotation (top), position (middle), and height (bottom) of the N_w = 1000 droplet center of mass above the local CNT center of mass as the CNT is driven by circularly polarized waves of ω = 208 GHZ at amplitudes ranging from A = 0.21 nm to A = 0.75 nm. Tangents between vertical lines indicate regions of surfing where the nanodroplet slides down the CNT surface.

dx.doi.org/10.1021/jz201614m | J. Phys. Chem. Lett. 2012, 3, 353−357

nanodroplet with N_w = 1000 transported by circularly polarized waves. The droplet and CNT form a coupled system where the CNT vibrates around its axis, and the droplet rotates around it (see Movies 1 and 2). We describe the droplet rotation around the *actual* position of the CNT by the angle θ of the vector pointing from the center of mass of a CNT segment local to the droplet to the actual droplet center of mass. The CNT segment is defined as a 2 nm section of the CNT bisected by the droplet. The time dependence of θ for different amplitudes A is in Figure 4 (top), the accompanied translation of the droplet along the CNT is in Figure 4 (middle), and the radial distance of the droplet from the CNT axis is in Figure 4 (bottom).

The droplet motion on the circularly polarized waves resembles *surfing*, where the droplet is sometimes grabbed better by the waves and for a while moves fast forward. At small waves, surfers cannot ride waves and neither can the droplet. This happens at A = 0.21 nm, where the vertical and longitudinal displacements of the droplet on the CNT are very small, as shown in Figure 4 (bottom) and (middle), respectively. Therefore, a small momentum is transferred to the water droplet which almost "bobs" in place like a "buoy", much like a surfer waiting for a wave. At larger amplitudes, the droplet can catch some of the waves and glide on them. We can see that at A > 0.45 nm, the droplet sometimes ($t \approx$ 125 and 700 ps) starts to progress forward quickly. The same is seen even better at the larger amplitudes, A = 0.54 nm and A = 0.75 nm, as denoted by the dotted tangential lines. In real surfing, the gravitational force of fixed spatial orientation accelerates the surfer on the traveling tilted wave. On the CNT, the gravitational force is replaced by the inertia forces acting on the nanodroplet surfing of the circularly polarized wave.

Temperature Effects. In Figure 5 (top), we also present the temperature dependence of the translational velocity of

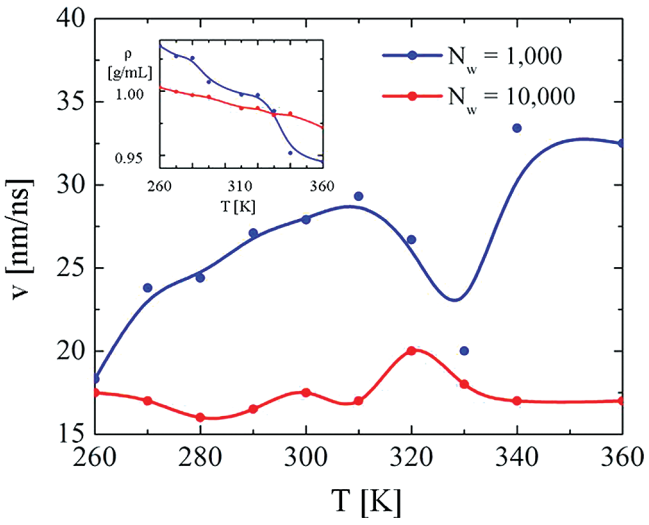

Figure 5. Temperature-dependent translational velocities, v, of the N_w = 1000 and 10 000 droplets transported by linearly polarized vibrational waves of ω = 208 GHz and A = 1.2 nm. (Inset) The temperature dependence of the effective nanodroplet density.

N_w = 1000 and 10 000 droplets, transported by linearly polarized waves of $\omega \approx$ 208 GHz and A = 1.2 nm. We can see that v increases with temperature for the small droplet, but it stays largely constant for the large droplet. In the region of T = 300−340 K, we can observe some anomaly, as in Figure 3. The effect is much more apparent for the N_w = 1000 droplet, where we can see a sharp slowing down of the droplet. By contrast, the larger droplet is accelerated here. This anomaly may be potentially linked with the reduced water densities in the droplets at higher temperatures (inset). At lower densities, the momentum transfer should be different, due to changed viscoelastic properties of the droplets. Although the droplets quickly evaporate molecules, sometimes also due to driving, they operate in saturated conditions inside small boxes allowing them to maintain a relatively stable number of molecules (5−10%).

In conclusion, we have demonstrated that TA vibrational waves on CNTs can translate/rotate nanodroplets adsorbed on their surfaces, as a function of the wave amplitude, polarization and frequency, the droplet size, and the temperature of the system. This material transport, which complements other transport methods at the nanoscale, could also be applied on planar surfaces, such as graphene. It has potential applications in molecular delivery,[39] fabrications of nanostructures,[40,41] and nanofluidics.[42]

■ ASSOCIATED CONTENT

Ⓦ Web-Enhanced Features

Movies showing nanodroplet transport along vibrated CNTs is available in the HTML version of this paper.

■ AUTHOR INFORMATION

Corresponding Author

*E-mail: pkral@uic.edu.

■ ACKNOWLEDGMENTS

We acknowledge NSF CBET support obtained under the grant CBET-0932812. J.R. would like to acknowledge support from the National Defense Science and Engineering Graduate Fellowship. B.W. would like to acknowledge the support from the Graduate Paaren Fellowship. The simulations were conducted with support from the Center for Nanoscale Materials (CNM), the National Energy Research Scientific Computing Center (NERC), and the National Center for Supercomputing Applications (NCSA).

■ REFERENCES

(1) Iijima, S. Helical Microtubules of Graphitic Carbon. *Nature* **1991**, *354*, 56−58.

(2) Saito, R.; Dresselhaus, G.; Dresselhaus, M. S. *Physical Properties of Carbon Nanotubes*; World Scientific Publishing Company: London, 1998.

(3) Král, P; Tománek, D. Laser-Driven Atomic Pump. *Phys. Rev. Lett.* **1999**, *83*, 5373−5376.

(4) Regan, B. C.; Aloni, S.; Ritchie, R. O.; Dahmen, U.; Zettl, A. Carbon Nanotubes as Nanoscale Mass Conveyors. *Nature* **2004**, *428*, 924−927.

(5) Svensson, K.; Olin, H.; Olsson, E. Nanopipettes for Metal Transport. *Phys. Rev. Lett.* **2004**, 145901.

(6) Wang, B.; Král, P. Coulombic Dragging of Molecules on Surfaces Induced by Separately Flowing Liquids. *J. Am. Chem. Soc.* **2006**, *128*, 15984.

(7) Wang, B.; Král, P. Dragging of Polarizable Nanodroplets by Distantly Solvated Ions. *Phys. Rev. Lett.* **2008**, *101*, 046103.

(8) Zhao, Y. C.; Song, L.; Deng, K.; Liu, Z.; Zhang, Z. X.; Yang, Y. L.; Wang, C.; Yang, H. F.; Jin, A. Z.; Luo, Q.; Gu, C. Z.; Xie, S. S.; Sun, L. F. Individual Water-Filled Single-Walled Carbon Nanotubes as Hydroelectric Power Converters. *Adv. Mater.* **2008**, *20*, 1772−1776.

(9) Schoen, P. A. E.; Walther, J. H.; Arcidiacono, S.; Poulikakos, D.; Koumoutsakos, P. Nanoparticle Traffic on Helical Tracks: Thermophoretic Mass Transport through Carbon Nanotubes. *Nano Lett.* **2006**, *6*, 1910−1917.

(10) Barreiro, A.; Rurali, R.; Hernandez, E. R.; Moser, J.; Pichler, T.; Forro, L.; Bachtold, A. Subnanometer Motion of Cargoes Driven by Thermal Gradients Along Carbon Nanotubes. *Science* **2008**, *320*, 775−778.
(11) Zambrano, H. A.; Walther, J. H.; Koumoutsakos, P.; Sbalzarini, I. F. Thermophoretic Motion of Water Nanodroplets Confined Inside Carbon Nanotubes. *Nano Lett.* **2009**, *9*, 66−71.
(12) Shiomi, J.; Maruyama, S. Water Transport Inside a Single-Walled Carbon Nanotube Driven by a Temperature Gradient. *Nanotechnology* **2009**, *20*, 055708.
(13) Insepov, Z.; Wolf, D.; Hassanein, A. Nanopumping Using Carbon Nanotubes. *Nano Lett.* **2006**, *6*, 1893−1895.
(14) Wang, Q. Atomic Transportation via Carbon Nanotubes. *Nano Lett.* **2009**, *9*, 245−249.
(15) Wang, Z.; Zhe, J. Recent Advances in Particle and Droplet Manipulation for Lab-on-a-Chip Devices Based on Surface Acoustic Waves. *Lab Chip* **2011**, *11*, 1280−1285.
(16) Hashimoto, H.; Koike, Y.; Ueha, S. Transporting Objects without Contact Using Flexural Travelling Waves. *J. Acoust. Soc. Am.* **1998**, *103*, 3230−3233.
(17) Kim, G. H.; Park, J. W.; Jeong, S. H. Analysis of Dynamic Characteristics for Vibration of Flexural Beam in Ultrasonic Transport System. *J. Mech. Sci. Technol.* **2009**, *23*, 1428−1434.
(18) Miranda, E. C.; Thomsen, J. J. Vibration Induced Sliding: Theory and Experiment for a Beam with a Spring-Loaded Mass. *Nonlinear Dyn.* **1998**, *19*, 167−186.
(19) Vielsack, P.; Spiess, H. Sliding of a Mass on an Inclined Driven Plane With Randomly Varying Coefficient of Friction. *J. Appl. Mech.* **2000**, *67*, 112−116.
(20) Long, Y. G.; Nagaya, K.; Niwa, H. Vibration Conveyance in Spatial-Curved Tubes. *J. Vib. Acoust.* **1994**, *116*, 38−46.
(21) Biwersi, S.; Manceau, J.-F.; Bastien, F. Displacement of Droplets and Deformation of Thin Liquid Layers Using Flexural Vibrations of Structures. Influence of Acoustic Radiation Pressure. *J. Acoust. Soc. Am.* **2000**, *107*, 661−664.
(22) Wixforth, A.; Strobl, C.; Gauer, C.; Toegl, A.; Scriba, J.; von Guttenberg, Z. Acoustic Manipulation of Small Droplets. *Anal. Bioanal. Chem.* **2004**, *379*, 982−991.
(23) Alzuaga, S.; Manceau, J.-F.; Bastien, F. Motion of Droplets on Solid Surface Using Acoustic Radiation Pressure. *J. Sound Vib.* **2005**, *282*, 151−162.
(24) Bennes, J.; Alzuaga, S.; Chabe, P.; Morain, G.; Cheroux, F; Manceau, J.-F.; Bastien, F. Action of Low Frequency Vibration on Liquid Droplets and Particles. *Ultrasonics* **2006**, *44*, 497−502.
(25) Jiao, Z. J.; Huang, X. Y.; Nguyen, N.-T. Scattering and Attenuation of Surface Acoustic Waves in Droplet Actuation. *J. Phys. A: Math. Theor.* **2008**, *41*, 355502.
(26) Mele, E. J.; Král, P. Electric Polarization of Heteropolar Nanotubes as a Geometric Phase. *Phys. Rev. Lett.* **2002**, *88*, 056803.
(27) Michalski, P. J.; Sai, N. A.; Mele, E. J. Continuum Theory for Nanotube Piezoelectricity. *Phys. Rev. Lett.* **2005**, *95*, 116803.
(28) Král, P.; Thanopulos, I.; Shapiro, M. Coherently Controlled Adiabatic Passage. *Rev. Mod. Phys.* **2007**, *79*, 53−77.
(29) Phillips, J. C.; Braun, R.; Wang, W.; Gumbart, J.; Tajkhorshid, E.; Villa, E.; Chipot, C.; Skeel, R. D.; Kale, L.; Schulten, K. Scalable Molecular Dynamics with NAMD. *J. Comput. Chem.* **2005**, *26*, 1781−1802.
(30) MacKerell, A. D. jr.; Bashford, D.; Bellot, M.; Dunbrack, R. L.; Evanseck, J. D.; Field, M. J.; Fischer, S.; Gao, J.; Guo, H.; Ha, S.; Joseph-McCarthy, D.; Kuchnir, L.; Kuczera, K.; Lau, F. T. K.; Mattos, C.; Michnick, S.; Ngo, T.; Nguyen, D. T.; Prodhom, B.; Reiher, W. E. III; Roux, B.; Schlenkrich, M.; Smith, J. C.; Stote, R.; Straub, J.; Watanabe, M.; Wiorkiewicz-Kuczera, J.; Yin, D.; Karplus, M. All-Atom Empirical Potential for Molecular Modeling and Dynamics Studies of Proteins. *J. Phys. Chem. B* **1998**, *102*, 3586−3617.
(31) Humphrey, W.; Dalke, A.; Schulten, K. VMD: Visual Molecular Dynamics. *J. Mol. Graph.* **1996**, *14*, 33−38.
(32) Vukovic, L.; Král, P. Coulombically Driven Rolling of Nanorods on Water. *Phys. Rev. Lett.* **2009**, *103*, 246103.
(33) Schneider, T.; Stoll, E. Molecular-Dynamics Study of Three-Dimensions One-Component Model for Distortive Phase Transitions. *Phys. Rev. B* **1978**, *17*, 1302−1322.
(34) Matsumoto, M.; Kunisawa, T.; Xiao, P. Relaxation of Phonons in Classical MD Simulation. *J. Therm. Sci. Technol.* **2008**, *3*, 159−166.
(35) Král, P. Linearized Quantum Transport Equations: AC Conductance of a Quantum Wire with an Electron−Phonon Interaction. *Phys. Rev. B* **1996**, *53*, 1103411050.
(36) Benumof, R. Momentum Propagation by Traveling Waves on a String. *Am. J. Phys.* **1982**, *50*, 20−25.
(37) Segal, D.; Král, P.; Shapiro, M. Ultraslow Phonon-Assisted Collapse of Tubular Image States. *Surf. Sci.* **2005**, *577*, 86−92.
(38) Bennes, J.; Alzuaga, S.; Ballandras, S.; Cherioux, F.; Manceau, J.-F. Droplet Ejector Using Surface Acoustic Waves. *IEEE Ultrasonics Symposium* **2005**, 823−826.
(39) Craighead, H. G. Future Lab-on-a-Chip Technologies for Interrogating Individual Molecules. *Nature* **2006**, *442*, 387−393.
(40) Baughman, R. H.; Cui, C. X.; Zakhidov, A. A.; Iqbal, Z.; Barisci, J. N.; Spinks, G. M.; Wallace, G. G.; Mazzoldi, A.; De Rossi, D.; Rinzler, A. G.; Jaschinski, O.; Roth, S.; Kertesz, M. Carbon Nanotube Actuators. *Science* **1999**, *284*, 1340−1344.
(41) Spinks, G. M.; Wallace, G. G.; Fifield, L. S.; Dalton, L. R.; Mazzoldi, A.; De Rossi, D.; Khayrullin, I. I.; Baughman, R. H. Pneumatic Carbon Nanotube Actuators. *Adv. Mater.* **2002**, *14*, 1728−1732.
(42) Schoch, R. B.; Han, J. Y.; Renaud, P. Transport Phenomena in Nanofluidics. *Rev. Mod. Phys.* **2008**, *80*, 839−883.